ISSN (Print) : 0974-6846
Indian Journal of Science and Technology, *Vol 8(26), DOI: 10.17485/ijst/2015/v8i26/82944, October 2015* ISSN (Online) : 0974-5645

A Study on Static and Fatigue Fractures on Tapered Double Cantilever Beam Specimen with Aluminum Foam through Simulation and Experiment

Hong Peng Sun[1] and Jae Ung Cho[2*]

[1]Department of Mechanical Engineering, Graduate School, Kongju National University, Seobuk-gu – 31080, Cheonan-si, Korea
[2]Department of Mechanical and Automotive Engineering, Kongju National University, Seobuk-gu – 31080, Cheonan-si, Korea; jucho@kongju.ac.kr

Abstract

Recently, the weight reduction and the safety are becoming important objectives at automotive engineering, and the materials used for automotive parts are transiting from steel and iron to plastic or multi-porous materials. In this study, aluminum foam is designed with the test specimen of TDCB shape. The shear fatigue strength is evaluated by being based on static behavior analysis under mode II conditions. The study results were verified through experimentation. The length and thickness of the TDCB test specimen models were 200mm and 25mm, respectively. As for the angle of the contact interface, 3 models were modeled, at 2° intervals from 6° to 10°. Examination of the results for the three models shows that under the same fatigue load conditions, the larger the tapered angle in the TDCB models, the longer the models are able to withstand the fatigue load. Also, in this study, using the finite element method, the adhesive strength against shearing fatigue load at the TDCB bonded structures with aluminum foam can be evaluated. It is thought that use of such verified analysis results is one method through which the structural safety of actual structures can be evaluated through analysis alone, without experimentation.

Keywords: Aluminum Foam, Adhesive, Equivalent Stress, Force Reaction, Fracture Behavior, Shear Mode, Tapered Double Cantilever Beam (TDCB)

1. Introduction

Recently, due to the need for energy savings, and in accordance with more stringent automotive laws and statutes, weight reduction and safety are becoming important objectives in automotive engineering, and the materials used for automotive parts are transitioning from steel and iron to plastic or multi-porous materials. Multi-porous materials such as expanded aluminum, Expanded Poly Propylene (EPP), and expanded polyurethane have low densities and are therefore quite light. They are being used in various fields, including automobiles and electronics, for the impact energy absorption, the sound absorption, and preventing vibration[1–3].

When structures made using composite materials are joined by welding, or using bolts and nuts in drilled holes, not only increase the processes and the time necessary for machining, but also increases weight. Also, in the case of aluminum foam, damage or deformation of the composite material may occur in the machining process or due to pressure from bolts and nuts. Due to these issues, recently, the use of bonded structures, wherein special adhesives such as epoxy bonds are used to join composite materials, is increasing. However, despite being engineered with sufficient rigidity and hardness, mechanical or bonded structures have been shown to be damaged by impact through various recent accidents. It is associated with rupturing of the contact face between composite materials due to foreign debris or defects in the bonded structure. Therefore, whereas manufacturers are giving consideration to the advantages of adhesives over previous joining technologies in terms of joining

* *Author for correspondence*

structures, as well as engineering components, the adhesive strength of parts joined by adhesives may be significantly reduced under impact loading conditions[4–6].

As it can be said to be important to study impact fatigue of bonded structures using composite materials, and the fracture toughness of the contact interface, in this study, the fatigue characteristics of bonded structures made of aluminum foam, a type of composite material with lighter weight and superior impact absorption and heat resistance than existing metal materials, were investigated. In accordance with the British industrial standards (British Standard; BS 7991) and the ISO international standards (ISO 11343), 3D modeling was conducted on test specimens made of aluminum foam composite material in the TDCB for the form of mode II. Also, using the ANSYS program, finite elements analysis was conducted to evaluate and verify the shear fatigue strength of aluminum foam bonded TDCB models. Also, in this study, in order to verify the results of analysis, aluminum foam with a closed cell structure made by Foam Tech Inc. of Korea was used to verify the evaluate the result of analysis[7–9].

2. Cohesive Zone Material Model and Study Model

As for the model in this study, the bilinear law for tangential traction and separation in cohesive zone materials was applied. Figure 1 shows that the relationship between load and displacement follows the OAC line. The triangular region under the OAC line indicates the critical fracture energy values.

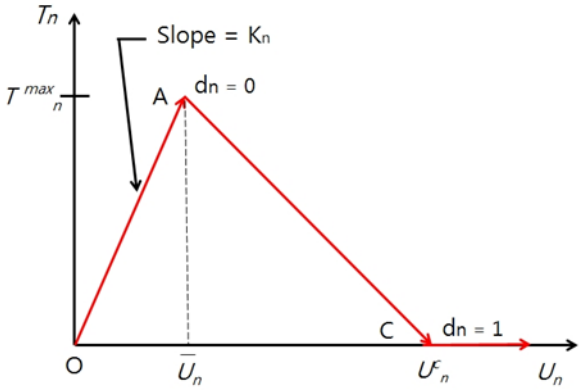

Figure 1. Contact stress of material with a bilinear cohesive zone.

The relation between tangential cohesive traction T_t and tangential displacement jump U_t can be expressed as formula (1)

$$T_t = K_t U_t (1-dt) \quad (1)$$

Where,

K_t=tangential cohesive stiffness $\frac{T_t^{max}}{\overline{U_t}}$

T_t^{max} = maximum tangential cohesive traction τ_{max}

$\overline{U_t}$ = tangential displacement jump at maximum tangential cohesive traction

U^c_t = tangential displacement jump at the completion of de-bonding

α = ratio of $\overline{U_t}$ *to* U^c_t

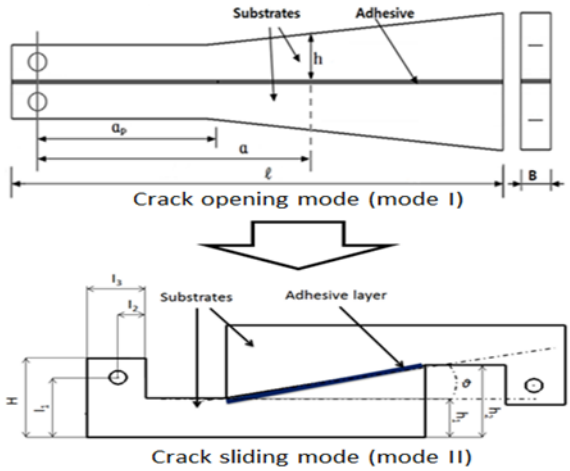

(a)

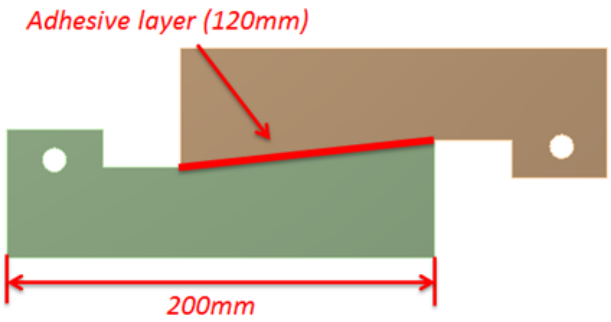

(b)

Figure 2. Configuration of model. (a) TDCB Specimen. (b) 2D Model (θ = 6°).

d_t = damage parameter associated with Mode II dominated bilinear cohesive law

The TDCB drawings specified in the British industrial standards were redesigned by using the single-lap joining method to suit this study. Figure 2(a) and (b) show the redesigned TDCB drawings, where the variable, θ, was the value for the taper angle of the TDCB test specimen. The length and thickness of the TDCB test specimen models were 200mm and 25mm, respectively. As for the angle of the contact interface, 3 models were made, at 2° intervals from 6° to 10°. As shown in Figure 2, whereas the angle at which the parts are joined varies from case to case, three representative study models were selected for analysis. Figure 3 is a photo of car body parts joined by using adhesive bonding[10–12].

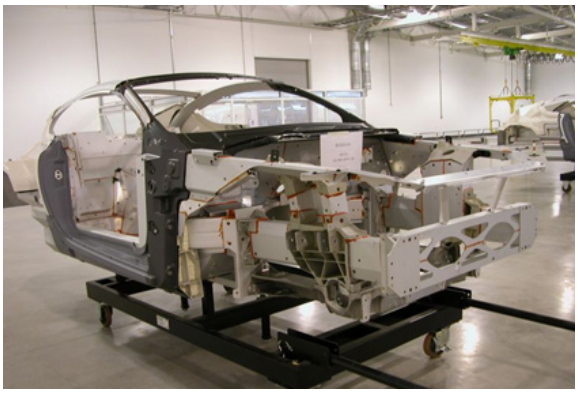

Figure 3. Car body with adhesive structure.

3. Static Testing Conditions and Test Results

3.1 Static Testing Conditions

The test device used in this study was the Landmark testing machine from MTS. The maximum force that can be applied to the specimens was 10kN. As an example, in Figure 4, the test device was set up by using the model with a taper angle of θ = 6°. The loading block on one side was locked in place with a cylindrical support. As for the beam on the opposite side, enforced shearing displacement was applied to the bottom load cell.

Figure 5 is a graph showing the data at the experimental process for the three types of test specimen, as well as reaction force according to displacement. At three curves, it can be seen that with every certain amount of displacement in the beam under the test specimen, the reaction force measured at the block increased by a certain amount. Among this data, the maximum reaction force for the specimen with the tapered angle of 10°, 220N, occurred, first, and, for the test specimen with the tapered angle of 6°, a maximum reaction force of 180N occurred in the last step.

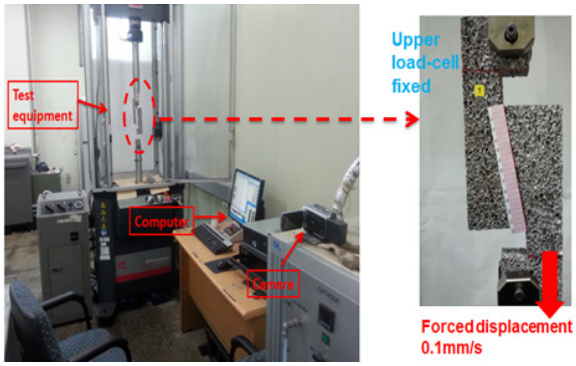

Figure 4. Experimental setup.

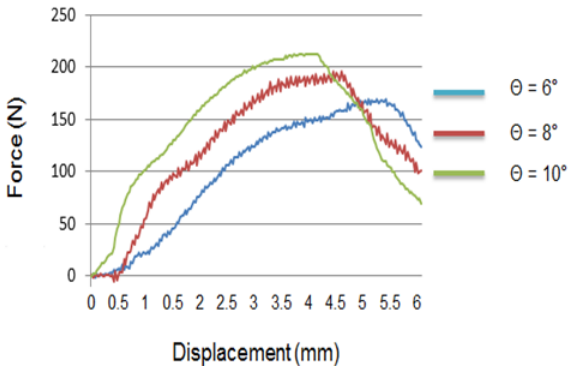

Figure 5. Experimental graphs of displacement-force reactions.

3.2 Fatigue Analysis Conditions

The finite element model for the aluminum foam, as shown in Figure 6, was divided into rectangular elements. The loading block on one side was locked in place using frictionless supports, while a fatigue load of 180N at 10Hz was applied to the loading block on the other side in the shearing direction. The value of fatigue load was gained through static testing, and was set to be lower than the maximum reaction load at each angle. While the fatigue load was being applied at 10Hz, displacement and load at each cycle as measured by the fatigue tester were obtained.

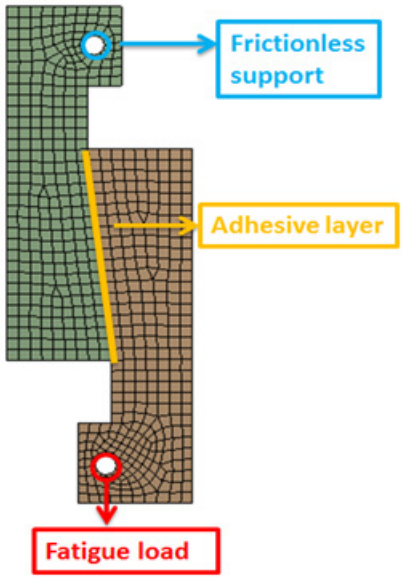

Figure 6. Boundary condition and mesh configuration (θ = 6°).

The material of the test specimen used in this study was Al-SAF40 aluminum foam. The material properties of the model used for analysis were as shown in Table 1[13–15].

Table 1. Material property

Property	Al-SAF40
Density (kg/m³)	400
Young's modulus (GPa)	2.374
Poisson's ratio	0.29
Yield strength (GPa)	1.8
Shear strength (GPa)	0.92

3.3 Results of Fatigue Analysis and Experimental Verification

Figure 7 shows the progress of the equivalent stress contours according to cycle by using the model with the tapered angle of 6°, under an 180N fatigue load at a fatigue cycle of 10Hz. As shown in the figure, the model maintains high stress when fatigue load is applied up to 3000 cycles. Examining the equivalent stress contour at 4000 cycles, it can be seen that equivalent stress almost disappears.

Figure 8 shows the correlation between load and displacement according to number of cycles. It can be seen that displacement rapidly increases from 0 cycles to approximately 100 cycles. After this, up to 3000 cycles, the shear displacement increased at regular intervals, but the equivalent stress was reduced. It can be said that at the adhesive interface, the slight damage occurred, weakening the adhesive strength. After approximately 4000 cycles, shear displacement again increased rapidly. It can be seen that after the progression of approximately 10mm displacement, the reaction force against adhesive strength also rapidly disappears.

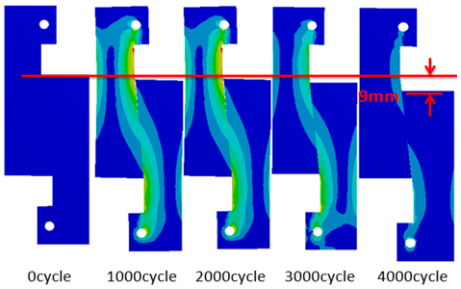

Figure 7. Procedures of equivalent stress contours at model with θ = 6°.

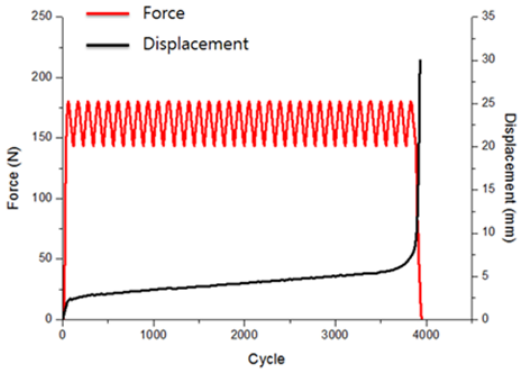

Figure 8. Graph of force and displacement due to cycle for θ = 6°.

The results for specimens with tapered angles of 8° and 10° were similar to the results for the test specimen with a the tapered angle of 6°. Figure 9 shows the displacement and reaction force under fatigue load for the specimen with the tapered angle of 8°. This graph shows that displacement rapidly increases when force is initially applied to the aluminum foam. However, whereas displacement rapidly changes before 100 cycles, it can be seen that the increase is consistent with the number of repetitions of the fatigue load after 100 cycles. Also, it can be seen that after the point where displacement increases to approximately 9mm, the fatigue load that the aluminum foam receives rapidly decreases. That is, it can be seen that adhesive strength of the aluminum foam disappears when fatigue load has been repeated for approximately 4500 cycles.

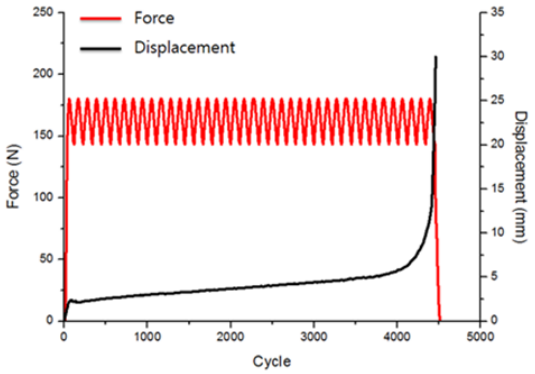

Figure 9. Graph of force and displacement due to cycle for θ = 8°.

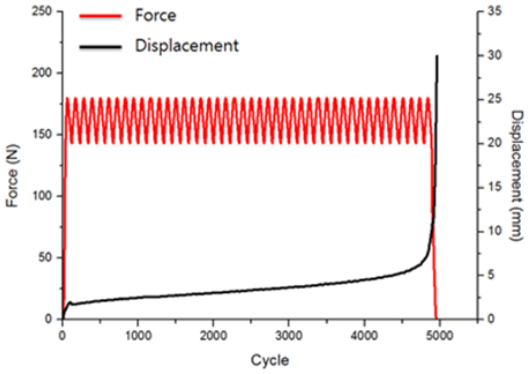

Figure 10. Graph of force and displacement due to cycle for θ = 10°.

Figure 10 shows the displacement and reaction force under the fatigue load for the specimen with the tapered angle of 10°. It can be seen that displacement rapidly increases from 0 cycles to approximately 100 cycles. Maximum reaction force has occurred at the point where displacement has progressed to approximately 2mm. Displacement increases in small increments from said point onwards. It can be seen that the adhesive strength disappears when the fatigue load has been repeated for approximately 5000 cycles, and displacement is approximately 9mm.

3.4 Experimental Verification of Analysis Data

To increase the reliability of analysis data, verification was performed. As shown in Figure 11, the results from experimentation and analysis were compared for the model with the tapered angle of θ = 6°. Examining the experimental process, it can be seen that the displacement of the lower test specimen increased gradually up to 3000 cycles of fatigue load, and that failure of the adhesive interface of the test specimen occurred at approximately 4000 cycles. It can be seen that the results from the experiment were similar to the analysis.

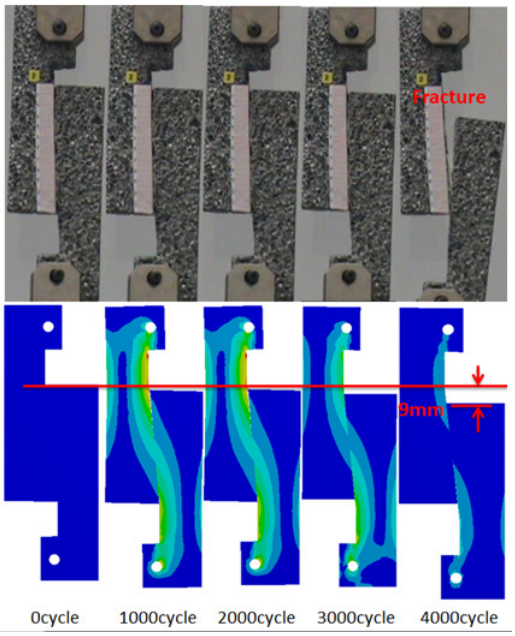

Figure 11. Comparison between fatigue configuration procedures of experiment and simulation for θ = 6°.

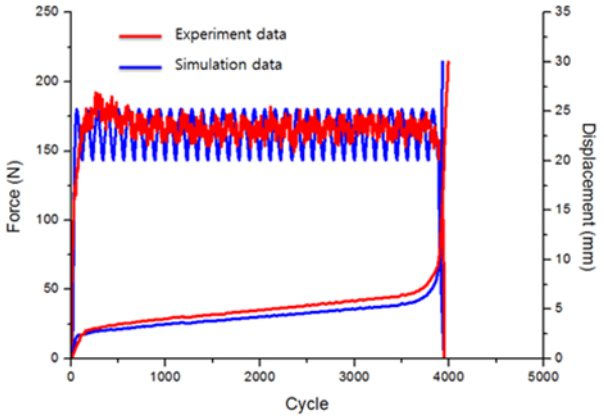

Figure 12. Comparison of graphs between fatigue procedures of experiment and simulation for θ = 6°.

The data from the above experimental and analysis processes are shown in the diagram in Figure 12. This graph shows that when displacement rapidly increases, load also increases dramatically. In the analysis data, it can be seen that the fatigue load is constant until complete separation from the adhesive interface. In

the experimental data, there was slight fluctuation with the repeated fatigue load. It can be said that for both experimental and analysis data, the complete yielding of the adhesive interface occurs when displacement due to the fatigue load progresses approximately 10mm. The data from analysis and tests are shown to be similar. Therefore, with a result of comparison between actual test data and analysis data, as analysis data had similar results as actual testing, the results from finite element analysis in this study were thought to be reliable.

4. Conclusion

After performing fatigue fracture analysis and experimental verification for bonded aluminum structures with different tapered angles, the following conclusions could be drawn.

- In the analysis results for the model with the tapered angle of 6°, the model maintains the high stress when the fatigue load is applied up to 3000 cycles. Examining the equivalent stress contour at 4000 cycles, it can be seen that the equivalent stress almost disappears.
- In the analysis results for the models with tapered angles of 8° and 10°, it can be seen that the adhesive strength of the aluminum foam disappears at approximately 4500 cycles and 5000 cycles of the fatigue stress, respectively.
- Comparing the graphs drawn using the analysis data for three models, it can be seen that, under the same fatigue loading conditions, the larger the tapered angle, the larger the number of cycles for which the fatigue load can be withstood.
- The comparison between actual test data and analysis data showed that results of analyses were similar to actual testing. Therefore, the results from the final element method employed in this study can be thought to be reliable. Applying this method, it is thought that it will be possible to investigate structural safety by using simulation only, instead of testing which is expensive and time-consuming.

5. Acknowledgement

This study was supported by the Basic Science Research Program through the National Research Foundation of Korea (NRF) grant funded by the Ministry of Education, Science and Technology (MEST) in 2011 (2011-0006548).

6. References

1. Kim DY, Kwak JH, Lee JH, Park KW, Jeong KY, Cheon SS. A study on the vibration analysis for the composite multi-axial optical structure of an aircraft. Journal of the Korean Society for Composite Materials. 2011; 24(2):14–21.
2. British Standard. Determination of the Mode I adhesive fracture energy G_{IC} of structure adhesives using the Double Cantilever Beam (DCB) and Tapered Double Cantilever Beam (TDCB) specimens. Imperial College of Science and Technology. 2001. p. 3–13.
3. Bang SO, Kim KS, Kim SH, Song SG, Cho JU. Study on compression test of aluminum foam and honeycomb sandwich composites. Journal of the Korea Academia-Industrial Cooperation Society. 2011; 12(9):3802–7.
4. Kim DB, Kim KW, Cho HY. Shape design of self-piercing rivet for joining dissimilar sheet metals. Journal of Korean Society of Mechanical Technology. 2012; 14:93–9.
5. Lee JK. Elastic analysis in composite including multiple elliptical fibers. Journal of the Korean Society for Composite Materials. 2011; 24(6):37–48.
6. Kim JG, Hwang YJ, Yoon SH, Lee DG. Improvement of the fracture toughness of adhesively bonded stainless steel joints with aramid fibers at cryogenic temperatures. Composite Structures. 2012; 94(9):2982–9.
7. Kim SS, Han MS, Cho JU, Cho CD. Study on the fatigue experiment of TDCB aluminum foam specimen bonded with adhesive. International Journal Precision Engineering and Manufacture. 2013; 14(10):1791–5.
8. Marzi S, Biel A, Stigh U. On experimental methods to investigate the effect of layer thickness on the fracture behavior of adhesively bonded joints. International Journal of Adhesion and Adhesives. 2011; 31(8):840–50.
9. Hart-Smith LJ. Further developments in the design and analysis of adhesive bonded structural joints. McDonnell-Douglas Co. 1980.
10. Choi HK, Cho JU. Study on the fatigue analysis of DCB model with aluminum foam. Journal of Korean Society of Mechanical Technology. 2012; 14(6):39–43.
11. Zhang YJ, Yang CS. FEM analyses for influences of stress-chemical solution on THM coupling in dual-porosity rock mass. Journal of Central South University. 2012; 19(4):1138–47.
12. Han MS, Choi HK, Cho JU, Cho CD. Experimental study on the fatigue crack propagation behavior of DCB Specimen with aluminum foam. International Journal Precision Engineering Manufacture. 2013; 14(8):1396–9.
13. Blackman BRK, Dear JP, Kinloch AJ, MacGillivray H, Wang Y, Williams JG, Yayla P. The failure of fiber composites and adhesively-bonded fibre composites under high rates of test Part III mixed-mode I / II and Mode II loadings. Journal of Materials Science. 1996; 31(17):4467–77.
14. Ohno N, Okumura D, Niikawa T. Long-wave buckling of elastic square honeycombs subject to in-plane biaxial compression. International Journal of Mechanical Sciences. 2004; 46(11):1697–713.
15. Sun J, Zhang L. Vehicle actuation based short-term traffic flow prediction model for signalized intersections. Journal of Central South University. 2012; 19(1):287–98.